

# Integrated Approaches for Global Warming Considering Water Environment Issues

Toshiharu Kojiri<sup>1</sup>

<sup>1</sup>*Disaster Prevention Research Institute, Kyoto University, Gokasho, Uji, Kyoto 611-0011, Japan*

## 1 INTRODUCTION

In Japan, about 1 degree-C rise of surface temperature has been monitored for this one century. Under the limited scenario simulation due to the global warming, 2 °C rise of temperature in 2050, 3 °C rise of temperature in 2100, and 10% increase of precipitation in global scale are estimated (IPCC 1). The precipitation in Canada, middle Europe and Siberia are increasing and in the tropical area in Africa is decreasing. The Elbe flood in 2002 was caused by the jet stream change and steady blocking phenomena. In Australia, the temperature is totally decreasing. Especially, the aridification in the East and the South-West and the precipitation increase in the South and Middle are estimated. In Japan, the fluctuation range of precipitation is getting bigger locally. The precipitation face to the Japan Sea in Hokuriku and Sanin is decreased and face to the Pacific Ocean in Tohoku and Kanto is increased caused by the change of monsoon in winter. Consequently, the winter is warmed with less snowfall and the severe storms are often generated due to the change of rain front and typhoon generation. From these viewpoints, the meteorological and hydrological dynamics against global warming and climate change can be analyzed by using the world-wide data through satellite from space, observation on ground, simulation in computer and so on. To understand the characteristics of drought event, special data of air temperature, sea surface temperature and precipitation in the Northern Hemisphere can be analyzed herein to estimate the future precipitation.

The water resources distribution becomes more confused because not only of meteorological (and hydrological) change of precipitation but also human activities in the developed or urbanized area. The countermeasures against these abnormal events are recognized from two approaches of hard and soft system. The hard system is to be built the control facilities to protect the property and human life, and the soft one is to inform the damage risk or to operate the facilities to reduce the disaster damage in advance. The considerable topics in water resources distribution are listed below;

- Spatial and temporal fluctuation of precipitation
- Impacts of runoff change to vegetation and ecosystem
- Water circulation change in global, regional and urban scales
- Flexible system for water resources management
- Conjunctive water resources with river, lake, ground water and so on
- New perspectives on water demand and consumption

## 2 RESENT RESEARCH APPROACHES ON IMPACT ASSESSMENT

### 2.1 Simulation procedures and conditions

#### 2.1.1 Hydrological conditions

The considered river basin is divided into small mesh cells with multi-layer (Kojiri *et al.*, 1998). The monthly temperature sequences are classified through ISODATA (Tou *et al.*, 1974). The daily temperature is generated around the extracted monthly temperature with random number obeying the obtained probability density function. For the daily precipitation, the precipitation generator is proposed by considering the durations of precipitation and non-precipitation, and the intensities of rainfall as shown in Fig. 1. Concretely, the following steps are taken;

- i) The monthly precipitation sequences for yearly unit are classified.
- ii) The temperature range is divided into several sub-ranges such as (-6 -9 -12 -15 -18 -21 -24 -27 -∞) and the durations of precipitation and non-precipitation are analyzed according to these sub-ranges.
- iii) The distribution function of daily precipitation is obtained under the conditional probability of temperature.
- iv) After extracting the monthly temperature, the precipitation duration is generated with random number.
- v) In the case of no-precipitation, the intensity is set as zero and otherwise, the precipitation is generated with random number.
- vi) The generation condition against statistical average and standard deviation are assumed as follows;

$$\mu - 0.5\sigma \leq \mu' \leq \mu + 0.5\sigma \quad (1)$$

The generated data out of these ranges are dismissed and new data is created until it will be inside of assumed range.

- vii) Applying the pattern classification for monthly precipitation data, the following objective function is

introduced;

$$D_j = \frac{1}{N_j} \sum \frac{|X_i - Z_j|}{Z_j} \rightarrow \min \quad (2)$$

where,  $Z_j$  is the cluster center  $j$ , and  $X_i$  is the sample data of monthly precipitation.

viii) Generating random number obeying the transition probabilities among yearly precipitation patterns, the next yearly pattern after the present situation is extracted.

ix) The necessary precipitation sequences are generated through the proposed iterations.

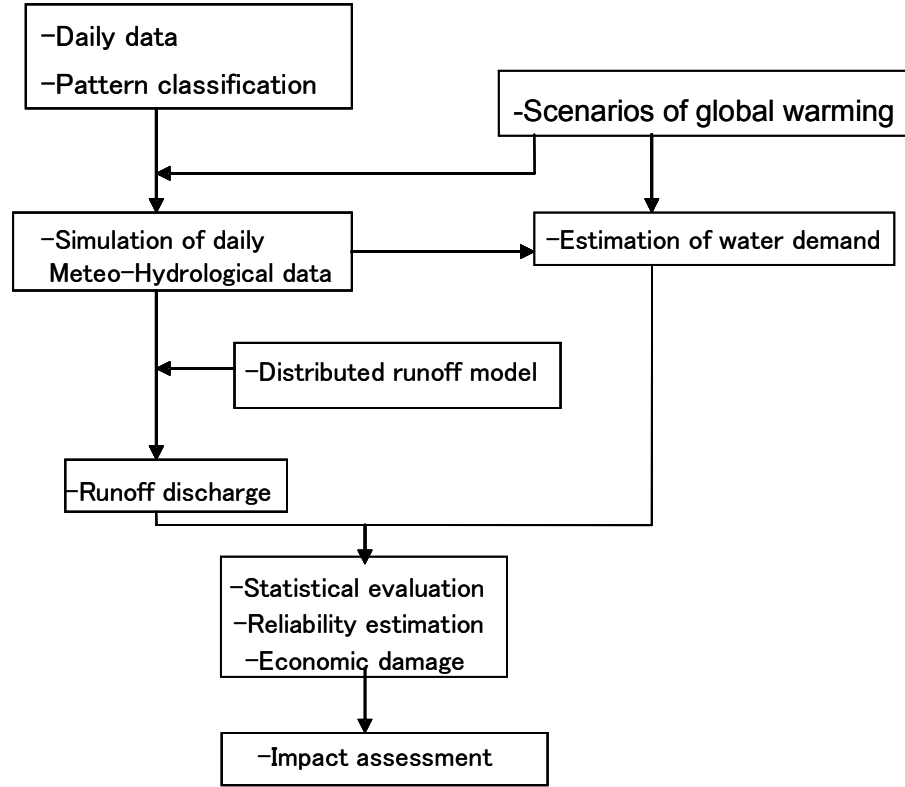


**Figure 1** Impact assessment procedures

### 2.1.1 Estimation of water demands

The necessary water demands of agriculture, industry and municipal water are estimated under the functions of temperature, precipitation, previous intake discharge volume after analyzing 20 years data as follows;

- Agriculture

$$\triangleright QA(t+1) = -0.03 - 0.01R(t-4) + 0.02T(t-4) + 0.83QA(t) + 0.14QA(t-2) \quad (3)$$

- Factory

$$\triangleright QF(t+1) = 0.10 + 0.67QF(t) - 0.10QF(t-1) + 0.10QF(t-2) + 0.14QF(t-3) \quad (4)$$

- Municipal

$$\triangleright QC(t+1) = 0.20 + 0.01T(t-4) + 0.63QC(t) + 0.09QC(t-1) + 0.09QC(t-2) \quad (5)$$

where,  $QA(t)$  is the intake water for agriculture at time  $t$ ,  $QF(t)$  is the intake water for factory (industry),  $QC(t)$  is the intake water for municipal activities,  $R(t)$  is the precipitation and  $T(t)$  is temperature.

### 2.1.3 Designated Scenarios for global warming

According to the first IPCC report, the following scenarios are designated herein;

- i) Same  $CO_2$  emission is kept for all periods.
- ii) In other case,  $CO_2$  increase is assumed with constant increase rate.
- iii) Temperature rise is set as  $\Delta T=3 \text{ } ^\circ C$  for global scale.

- iv) Temperature should affect the evapotranspiration processes.
- v) The land use situations are not changed with same runoff parameters.
- vi) Precipitation is set as three variations of  $\Delta P = (-10.0, 0.0, +10.0\%)$  though the precipitation increase in global scale way be evaluated as +2 to 9 %. After all, the following scenarios are set in Table 1.

Table 1 Applied scenarios for global warming

	$\Delta T$ degree-C	$\Delta P$
Case 1	$\pm 0$	$\pm 0\%$
Case 2	+3	$\pm 0\%$
Case 3	+3	+10%
Case 4	+3	-10%

The precipitation is generated with modified statistical parameters as follows;

$$\mu' = \mu + \Delta T \quad (6)$$

$$\sigma'^2 = \frac{\mu + \Delta T}{\mu} \sigma^2 \quad (7)$$

The average is changed according to the temperature rise and the standard deviation is obeyed with constant variability rule. Figures 2 and 3 show the number of continuous days for non-precipitation and for continuous days for precipitation under 3 °C raise and in designated sub-range in the applied river basin. In the case of temperature raise (Case 2), non-precipitation periods become shorter and continuous precipitation periods do longer. Though in this sub-range, precipitation moves less, in another sub-range (9-12 °C), precipitation from 20 mm to 40 mm seems to be get higher frequency. As, for the yearly precipitation, the specified area should get greater precipitation more than average due to the higher evapotranspiration in the area, the additional precipitation increase must be reasonable. The additional precipitation rate is allowed up to 4.5 % against 10 % increase and 3.6 % against -10 % increase cases.

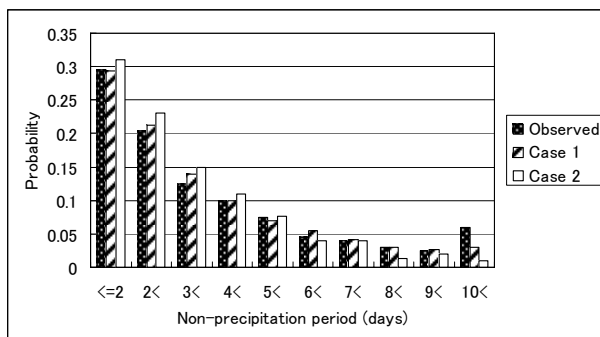


Figure 2 Comparison of number of days with non-precipitation

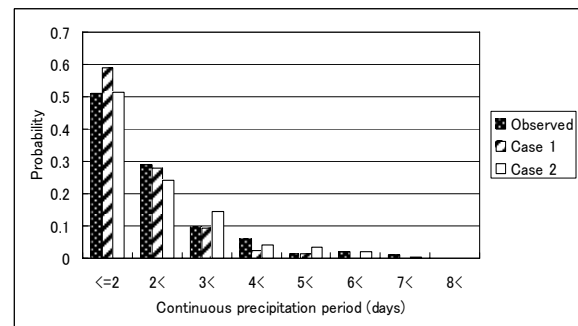


Figure 3 Comparisons of number of precipitation days with continuous precipitation

## 2.2 Assessed results for global warming

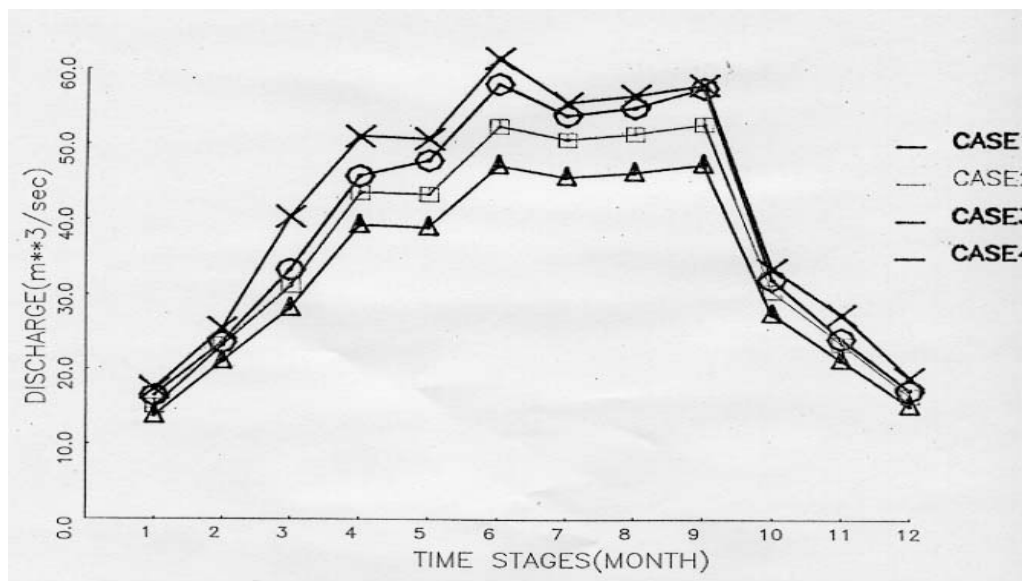
### 2.2.1 Hydrologic aspects

Table 2 shows the average and the standard deviation in sub-ranged temperature on the applied river basin. In Case 1, the temperature in lower sub-range is higher than on the monitored (present) case. In Case 2, the temperature in all sub-ranges is lower than in Case 1 and the precipitation becomes less. In all cases, higher temperature yields higher variation of precipitation.

Figure 4 shows the simulated results after 50 runs for designated scenarios. The symbol of circle mean Case1 ( $\Delta T = 0.0$  °C,  $\Delta P = \pm 0.0\%$ ), box does Case2 ( $\Delta T = +3.0$  °C,  $\Delta P = \pm 0.0\%$ ), cross is Case3 ( $\Delta T = +3.0$  °C,  $\Delta P = +10.0\%$ ), and triangle does Case4 ( $\Delta T = +3.0$  °C,  $\Delta P = -10.0\%$ ). The hydrograph in case 1 is bigger than other cases from February to May for 30 years from 1962 to 1992. The reason is that the sub-range of 3-15 degree-C got more precipitation of 30-50 mm range. The temperature raise of 3 °C will not bring big effects in water resources if the precipitation increase happens in more than 10 %.

**Table 2** Classified yearly precipitation distributions against sub-ranged temperature

	Monitor ed (present)		Case 1		Case 2		Case 3		Case 4		(mm)
Temperatu re Degree-C	Average	SD	Average	SD	Average	SD	Average	SD	Average	SD	
<= 6	2.22	6.01	2.8	8.53	2.74	8.22	3.23	8.51	2.64	6.97	
6< <=9	2.45	7.34	3.84	9.81	3.12	9.15	4.28	9.95	3.5	8.14	
9< <=12	4.73	12.12	4.99	13.04	3.82	7.3	5.88	14.45	4.81	11.82	
12< <=15	6.36	16.61	4.9	12.14	4.24	9.69	4.69	11.57	3.83	9.47	
15< <=18	7.05	17.93	7.15	18.19	5.43	11.95	7.78	17.75	6.37	14.52	
18< <=21	6.05	15.28	6.1	14.53	4.06	9.02	7.05	16.78	5.77	13.73	
21< <=24	9.16	21.92	7.69	15.64	9.81	22.25	9.18	18.75	7.51	15.34	
24< <=27	10.33	23.92	8.25	18.53	8.67	20.52	8.95	20.02	7.33	16.38	
27<	8.15	26.39	8.88	22.53	6.82	14.47	9.68	25.22	7.92	20.63	



**Figure 4** Comparison of simulated monthly hydrographs

Table 3 shows the hydro-statistical analysis for water resources events. The discharges of high water ( $Q_{95}$ ), Averaged water ( $Q_{185}$ ), low water ( $Q_{275}$ ) and drought water ( $Q_{355}$ ) are classified comparing Case 1. The discharge in Case 2 shows less water in the peak water area of 3 to 17 % decrease though not big change from high water to drought water. In Case 3, the discharge got higher with 5 to 14 % increase, especially, 14 % for high water and average water. In Case 4, the peak water becomes less with 14 to 25 % decrease and, the high and drought water decrease with 8 to 11 %.

**Table 3** Comparison of simulated discharge

	Case1	Case2	Case3	Case4	(m**3/day)
Q1	304	252(0.83)	321(1.05)	228(0.75)	
Q2	250	242(0.97)	264(1.06)	218(0.87)	
Q3	248	238(0.95)	262(1.05)	213(0.86)	
Q95	47	47(1.0)	53(1.13)	43(0.92)	
Q185	28	29(1.03)	32(1.14)	26(0.93)	
Q275	18	18(0.99)	20(1.08)	16(0.89)	
Q355	7	7(1.0)	8(1.09)	7(0.98)	

### 2.2.2 Reliability aspects

Reliability for water resources is evaluated through three factors of i) reliability, ii) resiliency and iii) vulnerability. Reliability presents the probability of drought event, resiliency does the continuity of drought, and vulnerability does the damage [Kojiri et al., 1987] under formulation as follows;

$$- \text{Reliability} = 1 - \text{drought number} / \text{total number of considered periods} \quad (8)$$

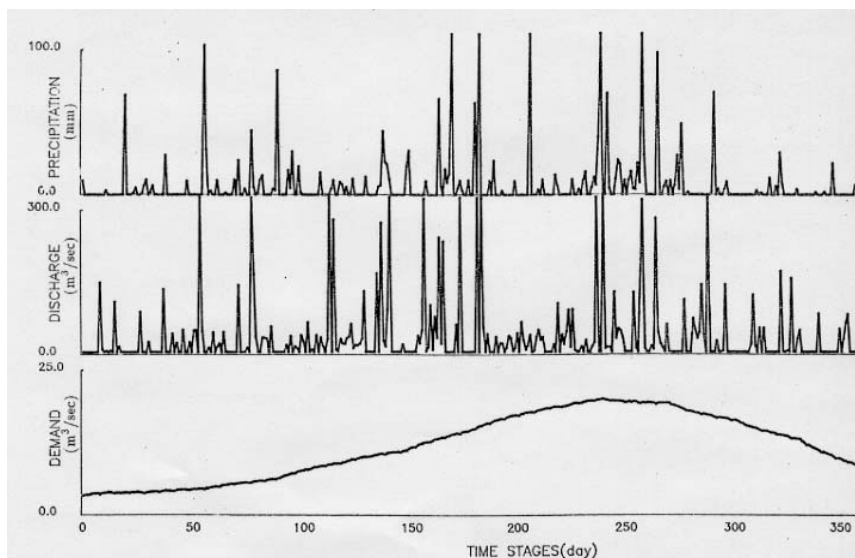
$$- \text{Resiliency} = \frac{1}{\text{total number of drought period} / \text{drought number}} \quad (9)$$

$$- \text{Vulnerability} = \frac{\sum f(1 - \text{drought index})}{\text{drought number}} \quad (10)$$

Drought index means social drought situation controlled by government or water authority and damage is calculated through the evaluated function such as square of deficit volume of water shortage.

**Table 4** Simulated results for reliability

	Drought number [/y]	Drought days [day]	Reliability	Resiliency	Vulnerability
Case1 (0, 0)	24	42	0.93425	0.5714	0.5450
Case2 (3, 0)	25	44	0.93150	0.5682	0.5504
Case3 (3, +10)	21	35	0.94247	0.6000	0.5081
Case4 (3, -10)	27	55	0.92876	0.3818	0.6026

**Figure 5** Applied precipitation, discharge and water demand sequences.

On the drought days, Case 1 has 42 and Case 2 does 22. Under the condition of 3 °C temperature raise, two days increases though vulnerability in Case 2 is bigger than Case 1. Case3 keeps 35 drought days and case 4 does 55 according to precipitation change. The drought numbers are 24, 25, 21 and 27 for each case, respectively.

On reliability, Case 1 and Case 2 show the same results through Case 3 is bigger and Case 4 is less. According to the precipitation increase, the drought probability may be reduced. In Case 2, Vulnerability and Resiliency become bigger than in Case 1, because the precipitation increase will provide bigger impact to drought situation in water resources than the temperature raise. Herein, the water deficit should be reformed as follows;

$$\text{Water shortage} = (1.0 - \text{Drought index}) \times (\text{Water demand at the necessary date}) \quad (11)$$

Figure 5 shows the simulated results on drought situation for past 50 years. As the peak of water demand was delayed from the discharge peak in the river, the drought happened after July, especially, in October and November strongly. If there are the big deficits in July, August and September, the catastrophic drought will follows in October and November. The drought number for periods from 294 to 298 is accounted as one in Case 4 and two in other cases. The drought number is not excellent factor to present drought severity without continuity and damage.

### 2.2.3 Economical aspects

Equivalent Variation approach (Morisugi *et al.*, 1985) is introduced to evaluate the economical drought damage in the river basin. The drought probability is assumed to be changed from  $P$  to  $P'$  due to the global warming. Then, the utility level should be changed from  $E[U_p(I)]$  to  $E[U_{p'}(I)]$ . The house or society should bare with this difference between utilities of  $E[U_p(I)]$  to  $E[U_{p'}(I)]$  under the future global warming, the difference can be recognized as the inevitable damage. In the following formulation, the drought probability is set as (1.0 – reliability) and Case 3 will not estimate the serious damage because of less drought probability.

$$E[U_p(I + EV)] = E[U_{p'}(I)] \quad (12)$$

where,

$$E[U_p(I + EV)] = P \cdot U(I + EV, x, 1) + (1 - P) \cdot U(I + EV, x, 0) \quad (13)$$

$$E[U_{p'}(I)] = P' \cdot U(I, x, 1) + (1 - P') \cdot U(I, x, 0) \quad (14)$$

The parameters of CES type applied here are already identified in the same river basin as follows;

$$\begin{aligned} h \cdot E[U] = & P \cdot [-(\rho/h) \{ \ln | W_1 x_1^{-\rho} + W_2 x_2^{-\rho} + W_3 (a_3 - x_3)^{-\rho} + W_4 (a_4 + x_4)^{-\rho} + W_5 (a_5 - x_5)^{-\rho} \\ & + W_6 (a_6 + x_6)^{-\rho} + W_7 (a_7 + x_7)^{-\rho} | \}] + (1 - P) \cdot [-(\rho/h) \{ \ln | W_1 x_1^{-\rho} + W_2 x_2^{-\rho} \\ & + W_3 (a_3 - x_3)^{-\rho} + W_4 (a_4 + x_4)^{-\rho} + W_5 (a_5 - x_5)^{-\rho} + W_6 (a_6 + x_6)^{-\rho} + W_7 (a_7 + x_7)^{-\rho} | \}] \end{aligned} \quad (15)$$

where,  $E[U]$  is the expected utility (10,000 Y-yen),  $h$  is the variance for identified error,  $W_i$  is the weight for each item,  $p$  is the parameter for alternated item,  $x_1$  is the monthly income (J-yen),  $x_2$  is the house space(m<sup>2</sup>),  $x_3$  is the commute time (min.),  $x_4$  is the sunshine hours per day (h),  $x_5$  is the dairy shopping (min),  $x_6$  is the public service (comfortable=1), and  $x_7$  is the risk for drought (drought=1 or non-drought=0). Inserting that  $P$  is the present drought probability and  $P'$  is the simulated results, the following results are obtained.

**Table 5** Estimated damage at house

	Damage (1,000 J-yen/house/y)	Damage (1,000 J-yen/house/y)
Case2 (3, 0)	2.7	0.23
Case3 (3, +10)	-8.4	-0.70
Case4 (3, -10)	5.5	0.46

As the drought probability increases with a little scale, the damage does not present big impacts where, 2,700 J-yen for Case 2 and 5.5000 J-yen for Case 4 per house. Table 6 shows the whole damage in the river basin, the water resources planning and utilization system against the serious drought due to the global warming year by year should be discussed in regional, river basin, national, international scales.

**Table 6** Estimated damage at the river basin

	Damage (1,000,000 J-yen/y)
Case2	490.8
Case3	-1526.9
Case4	999.8

## 3 DOWN SCALING FOR WATER RESOURCES WITH GCM OUTPTS

### 3.1 Calculation procedures for down scaling

Recently, many researches have considered the impacts of global warming and countermeasures on water

resources planning due to precipitation changes. Although the most popular information to analyze these impact assessments in global scale is the Coupled General Circulation Model (CGCM), (Tokioka et al., 1993), the resolution of CGCM of its output does not satisfy water resources researchers or planners. Even in CGCM developed by corroboration among CCSR, NIES and FRCGC, the horizontal resolution is about 100 km, which is not suitable for river basin management in Japan (Kimoto, 2005). Based on these viewpoints, we propose an effective downscaling approach to reduce the serious gap between CGCM and water resources management in river basins. First, downscaling approaches that combine a pattern classification and a weather generation are discussed. Second, meteorological patterns under global warming are extracted and third, precipitation in the river basin scale is estimated. Finally, hydrological characteristics in hourly units and 1-km resolution are carried out for water resources, as shown in Fig. 6.

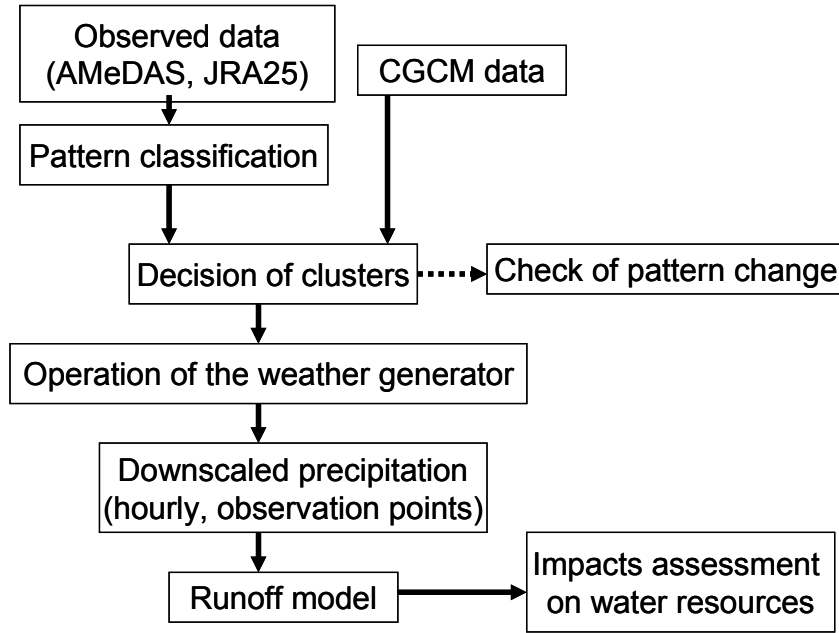


**Figure 6** Flowchart for proposed research.

Three Japanese organizations of CCSR, NIES and FRCGC have developed a new CGCM with the world's highest resolution in the world and re-produced 20<sup>th</sup> century's meteorological situation (hereafter, the 20<sup>th</sup>\_c. experiment) and simulated the future meteorological situation of the 21<sup>st</sup> century that reflects global warming (hereafter the 21<sup>st</sup>\_c. experiment). The global warming experiment was run under A1B and B1 scenarios in the Special Report on Emission Scenarios (SRES) provided by the Intergovernmental Panel on Climate Change (IPCC, 2007). Both experiments treated 30 years of data from 1979 to 2000 and from 2079 for 2100. Observed data are supplied by every six hours through JRA-25 (re-arranged data set) and AMeDAS from a North latitude of 15 degree to 55 degree and a East longitude from 105 degree to 155 degree with a resolution of 1.25 degree. ISODATA method is applied to classify the meteorological data of JRA25 and the precipitation data of AMeDAS (Kojiri *et al.*, 1989). Assume that  $x$  is a data property such as an observed point,  $Dat_t(x)$  is sample (observed) data for classification,  $S_m$  is data set of cluster  $m$ , and  $CL_m(x)$  is a cluster center. For the meteorological and hydrological data in this research, the output CGCM output is classified into suitable clusters with significant properties. The hydrological characteristics in the river basin scale should be extracted for the classified data set, and then future precipitation will be estimated with the weather generator.

Reasonable classification creates the proper cluster sets where the outputs of the considered experiments do not present big variation and fine discrimination between precipitation and no precipitation events is obtained. This definition is formulated as an average among calculated cluster centers and average among sample data of the 20<sup>th</sup>\_c experiment and cluster centers as follows;

$$E_{obs} = \frac{\sum_{i=1}^N OF_{i,m}}{N} \quad Dat_t \in S_m \quad (16)$$

$$E_{20} = \frac{\sum_{i=1}^N OF_{i,m}}{N} \quad Dat_t \in S_m \quad (17)$$

In the 21<sup>st</sup>\_c experiment, the same formula is introduced as follows;

$$E_{21} = \frac{\sum_{i=1}^N OF_{i,m}}{N} \quad Dat_t \in S_m \quad (18)$$

In cases where  $E_{obs}$ ,  $E_{20}$ , and  $E_{21}$  do not satisfy the following equations, the outputs of both experiments are dismissed;

$$2 \cdot E_{obs} > E_{20} \quad (19)$$

$$4 \cdot E_{20} > E_{21} \quad (20)$$

Among the un-dismissed extracted available data, significant data is decided based on significant rainfall patterns. Clusters that consist of less than thirty sample data are dismissed from this calculation process due to insufficient rainfall distribution accuracy. Assuming that  $N_{c,i}$  is the amount of cluster  $i$  data in classification  $c$ ,  $Nr_{c,i}$  is the amount of data with rainfall, and standard deviation  $\sigma_c$  of ratio of  $N_{c,i}$  and  $Nr_{c,i}$  is maximized for optimal classification as follows;

$$\begin{aligned} & \text{if } N_{c,i} > 30 \\ & \alpha_{c,i} = \frac{Nr_{c,i}}{N_{c,i}} \quad (21) \\ & \sigma_c = s(\alpha_{c,i}) \end{aligned}$$

### 3.2 Classified Results

We applied the proposed methodologies to two river basins. One is the Shiribetsu River which is located in Northern Japan in a cooler climate zone whose length and area are 126 km and 1640 km<sup>2</sup>. The upper area from the Nakoma point (1402.2 km<sup>2</sup>) is applied here. The other is the Gokase River located in Southern Japan in a warmer climate zone whose length and area are 106 km and 1820 km<sup>2</sup> applied to the upper area from the Miwa point (1044.1 km<sup>2</sup>). Since neither river has a storage reservoir in operation and both have necessary observation points, the simulated results can be compared from different viewpoints of water resources utilization. The sample data of JRA25 are transferred with Eq. (22) to be normalized in monthly units to reduce the sequential error of CGCM;

$$Obs_{m,t}^*(x,y) = \frac{Obs_{m,t}(x,y) - \frac{\sum_{i=1}^N Obs_{m,i}(x,y)}{N}}{\sqrt{\frac{\sum_{i=1}^N (Obs_{m,i}(x,y))^2}{N}}} \quad (22)$$

where,  $x$  is longitude,  $y$  is latitude,  $m$  is month,  $t$  is hour,  $Dat_{m,t}(x,y)$  are transferred data,  $Obs_{m,t}(x,y)$  is output of JRA25, and  $N$  is total amount of data. Since CGCM's grid apace in the 20<sup>th</sup>\_c. experiment is 1.125. which is different from JRA25 (1.25), the data are transferred with the following linear function;

$$\begin{aligned} GCM20_{m,t}(x,y) &= \sum_{i=1}^2 \sum_{j=1}^2 \frac{p_{i,j}}{P} Sim20_{m,t}(lon_i, lat_j) \\ p_{i,j} &= \frac{1}{\sqrt{(lon_i - x)^2 + (lat_j - y)^2}}, \quad i=1,2; j=1,2 \\ P &= \sum_{i=1}^2 \sum_{j=1}^2 p_{i,j} \end{aligned} \quad (23)$$

$$GCM20_{m,t}^*(x,y) = \frac{GCM20_{m,t}(x,y) - \frac{\sum_{i=1}^N GCM20_{m,i}(x,y)}{N}}{\sqrt{\frac{\sum_{i=1}^N (GCM20_{m,i}(x,y))^2}{N}}} \quad (24)$$

where,  $Sim20_{m,i}(x,y)$  is the output of the 20<sup>th</sup>\_c. experiment, and  $lon_i$  and  $lat_i$  are the nearest longitude and latitude from grid  $(x,y)$ . The output data of the 21<sup>st</sup>\_c. experiment are also transferred;

$$GCM21_{m,t}^*(x,y) = \frac{GCM21_{m,t}(x,y) - \frac{\sum_{i=1}^N GCM20_{m,i}(x,y)}{N}}{\sqrt{\frac{\sum_{i=1}^N (GCM20_{m,i}(x,y))^2}{N}}} \quad (25)$$

where,  $Sim21_{m,t}(x,y)$  is the output of the 21<sup>st</sup>\_c. experiment. Specific humidity of 850 hPa is recognized as reasonable meteorological data for the weather generator due to low correlations with precipitation.  $\chi^2$  qualification for the applied gamma function in the weather generator satisfies the high significance of 5% risk. Figure 7 shows the six-hour ahead precipitation at the Shiribetsu River and hourly distribution at Kuchan. Hourly precipitation is overestimated in the large probability range although basin precipitation distribution seems to show good results without wide variation.

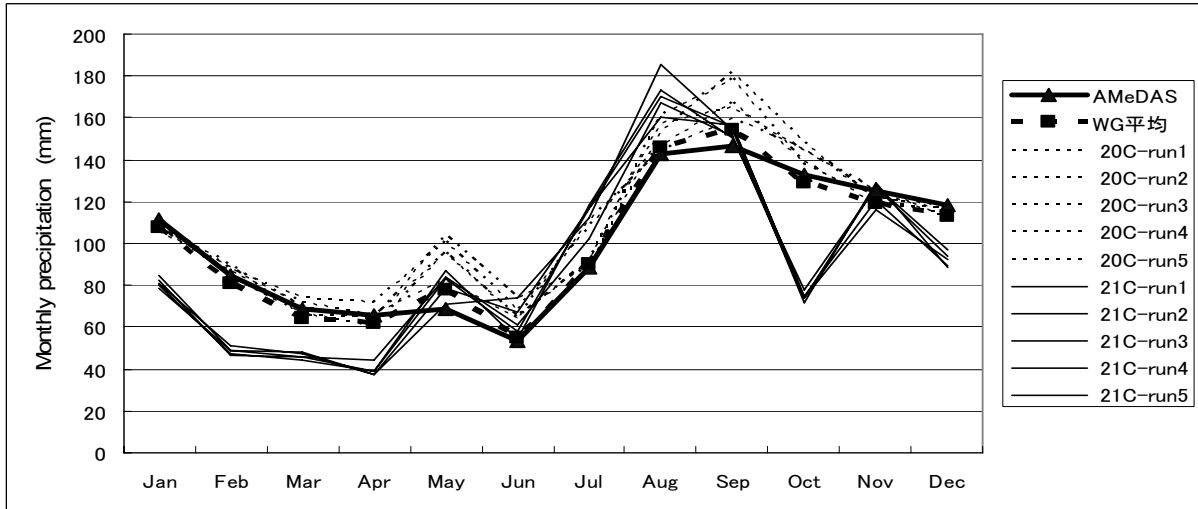


**Figure 7** Frequency distribution with the weather generator for 6-hour precipitation at Kuchan.

Figure 8 is the downscaled result at the Gokase River. The result of the 20<sup>th</sup>\_c. experiment underestimates the precipitation in summer due to less precipitation in June and July. Table 7 shows the difference of occurrence probabilities of precipitation. The North East type has a slighter occurrence probability than the others. In Japan, cold air repeatedly comes from the North and leaves for North. In the case of the South West type, cold air blows into the area and 500 hPa geopotential height comes down from normal height in the South and consequently the minimum point moves to South. The cold air generates the low air pressure which yields snowfall. On the other hand, although the North East type gets warm air and the corner of North East has the minimum value, the precipitation in Northern Japan does not occur easily.

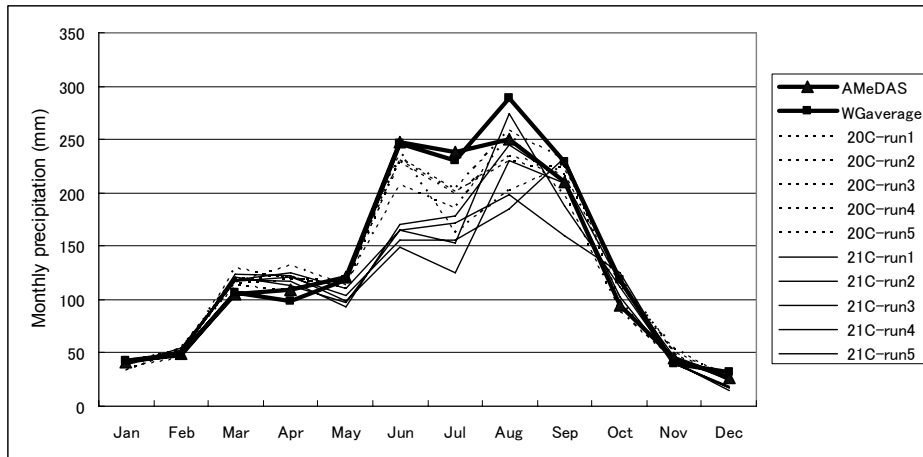


**Figure 8** Monthly precipitation after downscaling at the Gokase River Basin.

**Table 7** Re-classified results for rainfall occurrence probabilities.

	Number of clusters	Occurrence probability	Total data amount on JRA25	Total data amount on CGCM 20th_c	Total data amount on CGCM 21st_c
North East type	20	0.54	455	528	1542
South West type	27	0.88	1339	1269	455
Others	58	0.86	825	931	731

#### 4 FUTURE WATER RESOURCES WITH DISTRIBUTED RUNOFF MODEL

##### 4.1 Distributed Runoff Model

The distributed runoff model with 1-km mesh cells was applied (Kojiri et al., 1998). The number of meshes was 1525 for the Shiribetsu River and 977 for the Gokase River. Four direction and four layers system was developed. Figure 9 compares the rainfall distributions through the observed data (AMeDAS data), runoff discharge, precipitation, and snowmelt after downscaling at the Shiribetsu River. Rainfall is decided with a discrimination equation for air temperature. Runoff discharge from April to November decreases and the snowmelt peak goes down strongly.

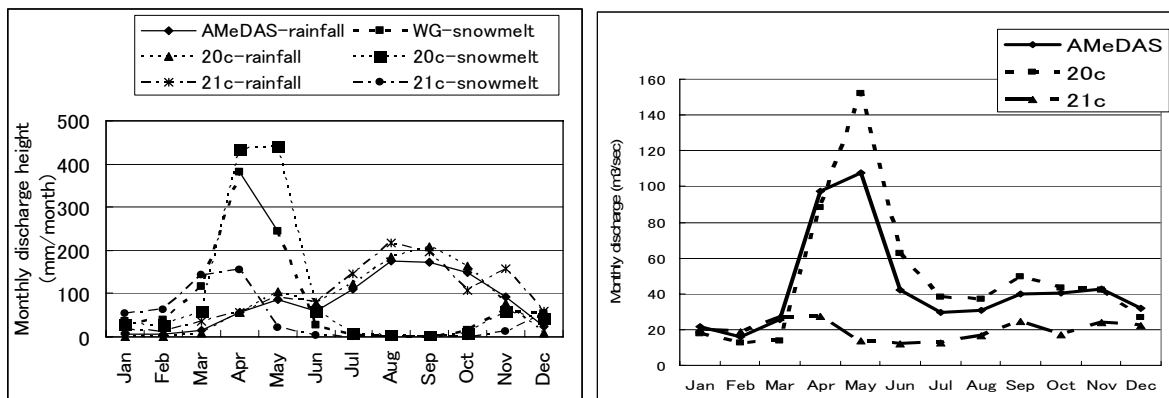


**Figure 9** Comparison of AMeDAS data, snowmelt, and rainfall (left), and discharge (right) at Nakoma in the Shiribetsu River.

Figure 10 compares the spatial distributions of snow depth from January to April. The snowmelt date clearly terminates earlier than the present situation in addition to snow depth reduction. Figure 8 presents the time sequences of the monthly maximum and monthly minimum discharges. The 20<sup>th</sup>\_c. experiment with downscaled data underestimates the discharge variation statistically. The 21<sup>st</sup>\_c. experiment generates larger peak discharge and less minimum discharge than the AMeDAS data

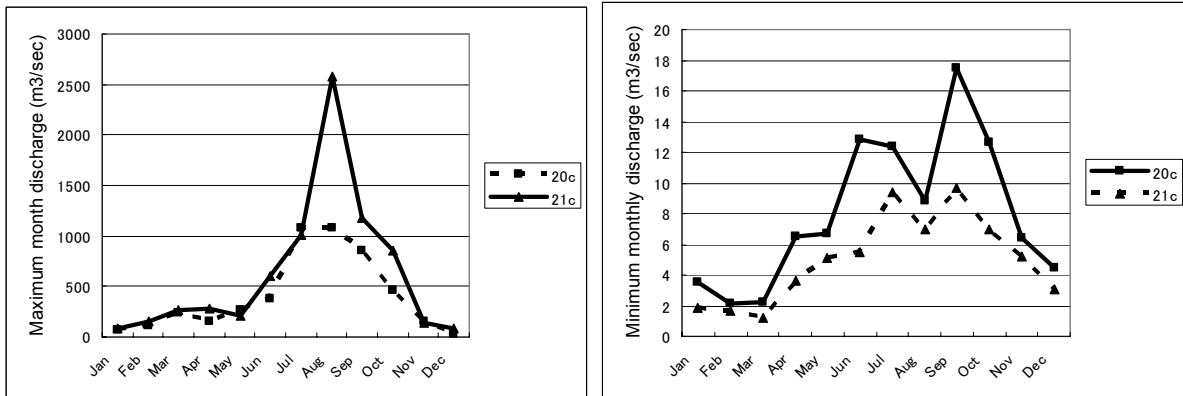


**Figure 10** Comparison of peak (left) and the lowest discharge (right) at Miwa in the Gokase River Basin.

## 5 CONCLUSIONS

The simple simulation generating daily meteorology and hydrology data with pattern classification is applied to evaluate the impact of global warming in the whole rice basin. The following results are summarized from water quantity to economical damage;

- i) Pattern classification approach combined with probabilistic statistical method is proposed. The daily data is generated with random number around the extracted feature pattern. The long term trend should be included to find next feature pattern under the conditional transition process.
- ii) The distributed runoff model is useful to grasp the runoff characteristics in the whole basin. The changing spatial land use patterns according to the social activities and economical development should be estimated through other methodologies.
- iii) In Japan, one scenario brings more water. The precipitation change in daily scale and monthly scale will take the important task to evaluate the allowable water resources utilization. The details DCM modeling suitable for above assessment procedures will be expected.
- iv) The economical damage is estimated by using drought damage formula. Case 4 ( $\Delta T=3$  degree-C,  $\Delta P=-10\%$ ) shows the biggest impacts in human life and  $\Delta P=10\%$  creates the enough precipitation to water resources in statistical viewpoint. The long trend of temperature raise and the concentrated heavy storms due to the global warming different from the past statistical records need more aggressive and perspective researches for human sustainability.

This paper proposed a downscaling approach that combined a pattern classification procedure and a weather generator with CGCM, JRA25 and AMeDAS data. Pattern changes on meteorological data due to climate changes were analyzed and precipitation changes were estimated in hourly units and 1- km resolution. The following results were obtained;

- Reasonable clusters were classified with the ISODATA method based on to the monthly occurrence probabilities of precipitation distributions in river basin.
- Practical hydrographs in hourly scale for both of whole river basins and observation points were re-produced and necessary accuracy downscaling with CGCM was obtained with the modified weather generator.
- In the Shiribetsu River Basin in the cooler climate zone, precipitation will decrease because the special meteorological event that chill breathes over this river basin will happen less frequently due to global warming. However, the heavy rainfall will fall frequently. As precipitation decreases in winter and snowmelt starts earlier than the present situation, runoff discharge will decrease in spring. On the other hand, discharge will decrease in summer due to evapotranspiration increase.
- In the Gokase River Basin in the warmer climate zone, the precipitation in June and July will decrease

because no rainfall periods in the rainy season increase. Consequently, as the discharge variation increases, such natural disasters as flood and drought will happen more frequently.

## REFERENCES

- Intergovernmental Panel on Climate Change (2007): *Climate Change 2007: The Physical Science Basis*, Contribution of Working Group I to the Fourth Assessment Report of the IPCC (available at <http://ipcc-wg1.ucar.edu/wg1/wg1-report.html>).
- Kimoto M. (2005): *Simulated change of the east Asian circulation under global warming scenario*, Geophys. Res. Lett., 32, L16701, doi:10.1029 / 2005 GL 023383.
- Kojiri, T. and Unny, T.E. (1989): *Application of Classification Techniques to Hydrological Data*, J. Japan Soc. Hydrol. & Water Resour., Vol.2, No.1, pp.53-59.
- Kojiri, T., Tokai, A. and Kinai, Y. (1998): *Assessment of River Basin Environment through Simulation with Water Quality and Quantity*, Annuals of Disas. Prev. Res. Insti., Kyoto University., No.41 B-2, pp.119-134.
- Morisugi, S. and Ooshima, N. (1985) Proposal of Evaluation Procedures to get the un-preferable benefit at individual house due to the decrease of drought probability, Proc. JSPS, Jr. of trans., No.359, IV-3, 99-98.
- Tokioka, T., Yamazaki, M. and Sato, N. (1993): *Numerical Simulation for Climate Model*, Press of University of Tokyo.
- Tou, J.T. and Gonzalez, R.C. (1974): *Pattern Recognition Principle*, Addison-Wesley Publishing Company, Applied Mathematics and Computation, No.2, pp.94-109.